Published in final edited form as:
J Am Chem Soc. 2009 March 25; 131(11): 3798–3799. doi:10.1021/ja806064t.

Intermolecular Electron-Transfer Catalyzed on Nanoparticle Surfaces

Adrienne M. Carver[a], **Mrinmoy De**[a], **Halil Bayraktar**[a], **Subinoy Rana**[a], **Vincent M. Rotello**[a,b], and **Michael J. Knapp**[*,a,b]

a*Department of Chemistry, University of Massachusetts, Amherst, Massachusetts 01003, USA*

b*Program in Molecular and Cellular Biology, University of Massachusetts, Amherst, Massachusetts 01003, USA*

Abstract

Surface-functionalized nanoparticles enhance the rate of electron transfer (ET) between Cyt *c* (Fe^{2+}) and $Co(phen)_3^{3+}$ by a factor of 10^5 through simultaneous electrostatic binding of ET donor and acceptor.

Interprotein electron transfer (ET) is crucial to energy transduction in photosynthesis and respiration, and is a direct example of protein recognition coupled with chemistry. The effects of distance and driving force are well understood, and can be manipulated in synthetic and natural systems to enhance ET kinetics.[1,2] In contrast, the effects of surface binding and dynamics on ET rates are harder to interpret,[3-6] making new model systems crucial for understanding the role of dynamics in ET reactivity.

Nanoparticles are capable of catalyzing selected reactions, by acting as artificial receptors for substrates.[7,8] For example, the rates of peptide ligation[7] and phosphodiester cleavage were enhanced by up to 10^3–fold on functionalized nanoparticle surfaces.[9] Here, we show a 10^5-fold enhancement of an intermolecular ET rate through use of surface-functionalized nanoparticles (**Au-TX**) as artificial receptors. This catalysis arises through bringing ET donor and acceptor into close proximity, demonstrating the ability to modulate protein ET at surfaces, and provides a tool for observing and controlling the interplay between binding, dynamics, and reactivity.

Bimolecular ET kinetics follow Marcus theory,[2] with driving force, reorganization, and steric factors determining rate. Cytochrome *c* (Cyt *c*) undergoes rapid ET with other proteins, as well as with small molecules. The dominant ET pathway is over the exposed heme edge; however heme access is limited by surface Lys residues,[10] making ET selective for partners that have the appropriate binding surface.

Au nanoparticles functionalized with thiol ligands containing the free-carboxylate form of amino acids (**Au-TX**)[8] bind to Cyt *c* (pI = 10) with $K_S \sim 10^7\ M^{-1}$. [11,12] Moreover **Au-TX** binds selectively to the surface of Cyt *c* near the heme edge.[11] As the charges of both $Co(phen)_3^{3+}$ and Cyt *c* are complementary to that of **Au-TX**, we tested whether concurrent binding could catalyze ET. The kinetic scheme accounting for the pre-equilibrium binding of Cyt *c* to **Au-TX**, followed by $Co(phen)_3^{3+}$ binding (K_D) and ET (k_{ET}):

Fax: 413-545-4490; Tel: 413- 545-4001, E-mail: E-mail: mknapp@chem.umass.edu.

Supporting Information **Available:** Additional kinetics and calorimetric data. This material is available free of charge via the Internet at http://pubs.acs.org.

$$\text{Cyt c}^{2+} + \text{Au–TX} \overset{K_S}{\rightleftharpoons} \text{Cyt c}^{2+}\text{:Au–TX} + \text{Co(phen)}_3^{3+} \overset{K_D}{\rightleftharpoons} \overset{k_{ET}}{\longrightarrow} \quad (1)$$

Cyt *c* was reduced with dithionite followed by gel filtration, and $Co(phen)_3^{3+}$ synthesized as per the literature. Cyt *c* oxidation was monitored as a single exponential decrease in A_{550} following the mixing of Cyt *c* (5 μM after mixing, 10mM Tris, pH 7.40, I = 20 mM, 12 mM NaCl) with $Co(phen)_3^{3+}$ (0.083 – 1.00 mM after mixing, in same buffer) in a stopped-flow spectrometer. Cyt *c* oxidation by $Co(phen)_3^{3+}$ was nearly independent of $[Co^{3+}]$, with k_{ET} = 0.66 (±0.02) s^{-1} (Figure 2),[13] in good agreement with prior reports.[14] This has been attributed to a rate-limiting conformational change at the heme edge of Cyt *c*; however, under moderate ionic strength the bimolecular ET rate is $k_{ET}/K_D = 10^3\ M^{-1}\ s^{-1}$.[15]

The Cyt *c*:**Au-TAsp** adduct was formed by pre-incubating Cyt *c* (10 μM) with **Au-TAsp** (0.16 – 1.04 μM; higher concentrations were not used due to high optical density), then mixing with $Co(phen)_3^{3+}$ as above. Cyt *c*:**Au-TAsp** oxidation was evident as single-exponential decays in A_{550}, indicating that Cyt *c* binding to **Au-TAsp** was in a rapid pre-equilibrium (Eq. 1). As the position of this equilibrium favored unbound Cyt *c*, the ET process may be considered as coupled.[16] The observed rates for Cyt *c*:**Au-TAsp** exhibited saturation due to $Co(phen)^{3+}$ binding, with k_{obs} as high as 65 s^{-1} (Figure 2). Analogous data sets for Cyt *c*:**Au-TPhe** exhibited similar saturation kinetics.[13] The second order kinetics were fitted to obtain apparent rate constants for Cyt *c* oxidation: $k_{obs} = k_{ET(app)}[Co]_0/([Co]_0+K_D)$.

The apparent maximum ET rate, $(k_{ET})_{app}$, was a linear function of nanoparticle concentration, indicating that the binding of Cyt *c* to **Au-TX** (K_S of Eq. 1) was far from equilibrium (Figure 3). Under rapid pre-equilibrium conditions, (k_{ET}/K_S)[**Au-TX**] = $(k_{ET})_{app}$; the slope of Figure 3 is the absolute bimolecular rate constant for $Co(phen)_3^{3+}$ reacting with Cyt *c* on the **Au-TX** surface. Linear least-squares fitting for Cyt *c*:**Au-TX** (X = Asp, Phe) yielded slopes that were nearly identical: k_{ET}/K_S = 1.35 (±0.03) × 10^8 and 1.20 (±0.03) × $10^8\ M^{-1}\ s^{-1}$, respectively. This is significantly larger than the ET rate in the absence of **Au-TX** ($1 \times 10^3\ M^{-1}\ s^{-1}$),[15] indicating that complexation by **Au-TX** catalyzed the ET reaction by 10^5.

This catalysis can be understood within the context of Marcus theory,[2] which states that the rate of bimolecular ET depends on the collision rate ($Z \sim 1 \times 10^{11}\ M^{-1}\ s^{-1}$) and the activation energy (ΔG^*): $k = Z\exp(-\Delta G^*/RT)$. In the limit of low driving force ($\Delta G^0 \ll \lambda$), $\Delta G^* = \lambda/4 + w$, where w is the work to bring the reactants together. The reaction of Cyt *c*(Fe^{2+}) with $Co(phen)_3^{3+}$ ($k = 1 \times 10^3\ M^{-1}\ s^{-1}$) can be attributed to λ = 44 kcal/mol, assuming that w = 0. This λ is consistent with the self-exchange reaction rate for each reagent.[2] The faster rate in the presence of **Au-TX** may arise from changes in either λ or w; should λ remain unchanged, the data could be accommodated with w = - 7 kcal/mol. This value for work is attributed to the electrostatic attraction of $Co(phen)_3^{3+}$ and Cyt *c* to **Au-TX**.

This electrostatic attraction increases the local concentration of each reagent. Calorimetric and kinetic data indicate that the $Co(phen)_3^{3+}$:**Au-TX** binding equilibrium was saturated at 1 mM $[Co(phen)_3^{3+}]$, leading to the plateau in k_{obs} (Figure 2); in contrast, Cyt *c* binding to **Au-TX** was sub-saturating, leading to the linear dependence of k_{ET} on [**Au-TX**] (Figure 3). Entropic factors (i.e. the "Circe effect"[17]) presumably dominate intermolecular ET catalysis in the Cyt *c*:**Au-TX** system, however enthalpic contributions cannot be excluded.

Kinetic complexity masked the rate of electron flow within encounter complexes in previous studies of the relationship between conformational dynamics and interprotein ET. In some cases, the overall rate was limited by a conformational change, leading to gated ET.[16,18,19] In other cases, ET was rate-limiting but occurred following a disfavored conformational change

with concomitant coupled ET.[3,4] Although amide H/D exchange showed that **Au-TPhe** bound to a smaller Cyt *c* face than **Au-TAsp**,[11] which could increase the rate of conformational dynamics, this did not translate into faster ET kinetics for Cyt *c*:**Au-TPhe**. This suggests that conformational dynamics within the {Cyt *c*:**Au-TX**:Co^{3+}} encounter complex are much faster than ET, and that dynamics may be uncoupled from ET under these conditions.

In summary, we have demonstrated the use of nanoparticles as highly efficient catalysts for intermolecular ET. These catalysts function by reversibly binding the ET donor and acceptor, thus increasing the local concentration of the redox partners. This process may provide a model for understanding intermolecular ET, in which binding is coupled to reactivity.

Supplementary Material

Refer to Web version on PubMed Central for supplementary material.

Acknowledgements

We thank the Graduate Council for a fellowship (HB), the NIH (GM077413, MJK; GM077173, VMR) for funding, and Prof. M. Maroney for instrument access.

References

1. Gray HB, Winkler JR. Annu Rev Biochem 1996;65:537–561. [PubMed: 8811189]
2. Marcus RA, Sutin N. Biochim Biophys Acta 1985;811:265–322.
3. Kang SA, Crane BR. Proc Natl Acad Sci USA 2005;102:15465–15470. [PubMed: 16227441]
4. Liang ZX, Kurnikov IV, Nocek JM, Mauk AG, Beratan DN, Hoffman BM. J Am Chem Soc 2004;126:2785–2798. [PubMed: 14995196]
5. Groves JT, Fate GD, Lahiri J. J Am Chem Soc 1994;116:5477–5478.
6. Liu T, Zhong J, Gan X, Fan CH, Li GX, Matsuda N. ChemPhysChem 2003;4:1364–1366. [PubMed: 14714390]
7. Fillon Y, Verma A, Ghosh P, Ernenwein D, Rotello VM, Chmielewski J. J Am Chem Soc 2007;129:6676–6677. [PubMed: 17488077]
8. You CC, De M, Han G, Rotello VM. J Am Chem Soc 2005;127:12873–12881. [PubMed: 16159281]
9. Manea F, Houillon FB, Pasquato L, Scrimin P. Angew Chem Int Edit 2004;43:6165–6169.
10. Cytochrome c. Univ Sci Books; Sausalito, CA: 1996.
11. Bayraktar H, You CC, Rotello VM, Knapp MJ. J Am Chem Soc 2007;129:2732–2733. [PubMed: 17309259]
12. Marini MA, Marti GE, Berger RL, Martin CJ. Biopolymers 1980;19:885–898.
13. Supplemental Material
14. Rush JD, Koppenol WH, Garber EAE, Margoliash E. J Biol Chem 1988;263:7514–7520. [PubMed: 2836388]
15. Holwerda RA, Knaff DB, Gray HB, Clemmer JD, Crowley R, Smith JM, Mauk AG. J Am Chem Soc 1980;102:1142–1146.
16. Davidson VL. Acc Chem Res 2000;33:87–93. [PubMed: 10673316]
17. Jencks, WP. Adv Enzymol Relat Areas Mol Biol. Meister, A., editor. Vol. 43. John Wiley & Sons; 1975. p. 219-410.
18. Mei HK, Wang KF, Peffer N, Weatherly G, Cohen DS, Miller M, Pielak G, Durham B, Millett F. Biochemistry 1999;38:6846–6854. [PubMed: 10346906]
19. Pletneva EV, Fulton DB, Kohzuma T, Kostic NM. J Am Chem Soc 2000;122:1034–1046.

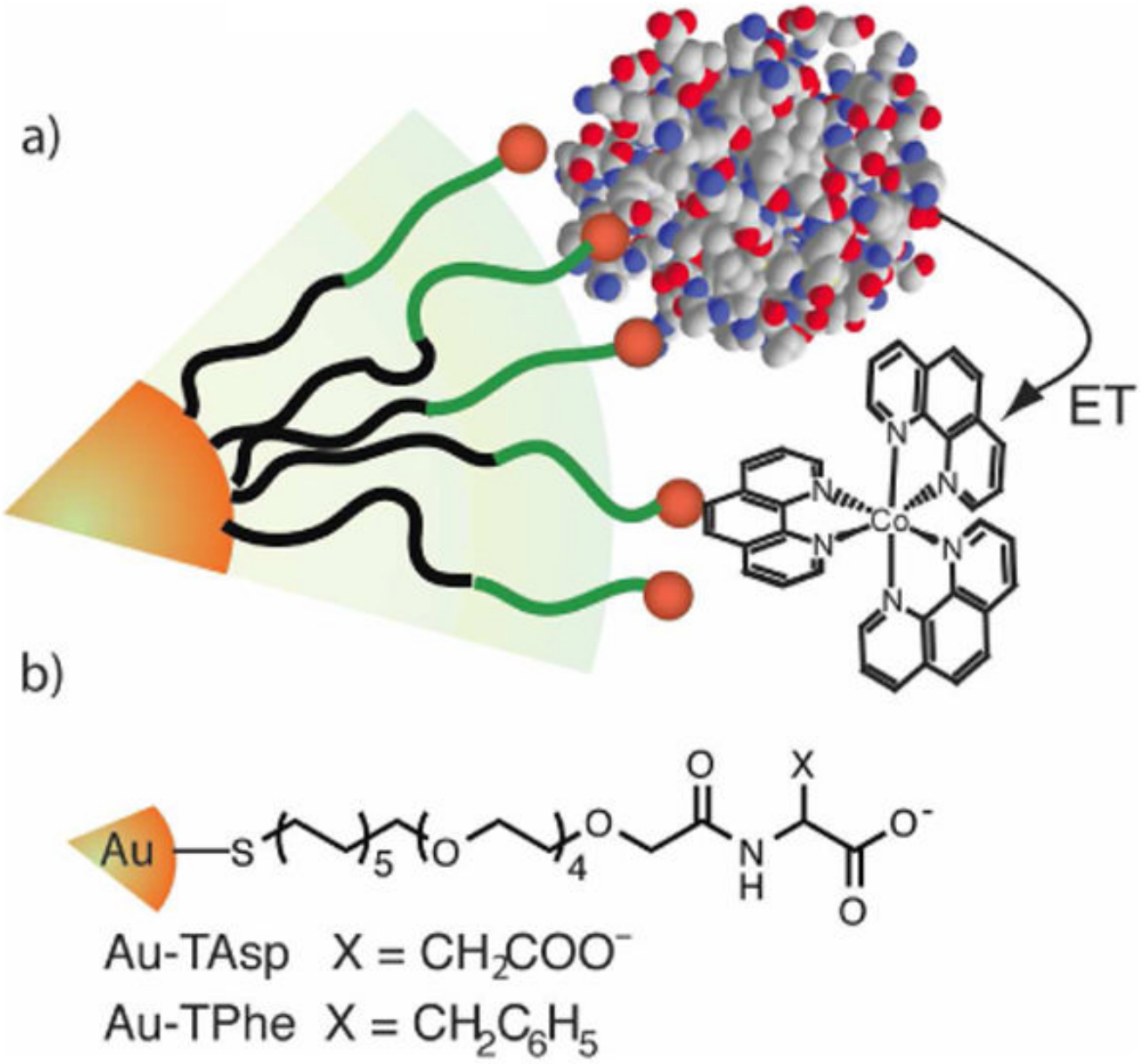

Figure 1.
a) Encounter complex for election transfer from Cyt *c* to $Co(phen)_3^{3+}$ on the surface of **Au-TX**; b) structure of **TX** ligands.

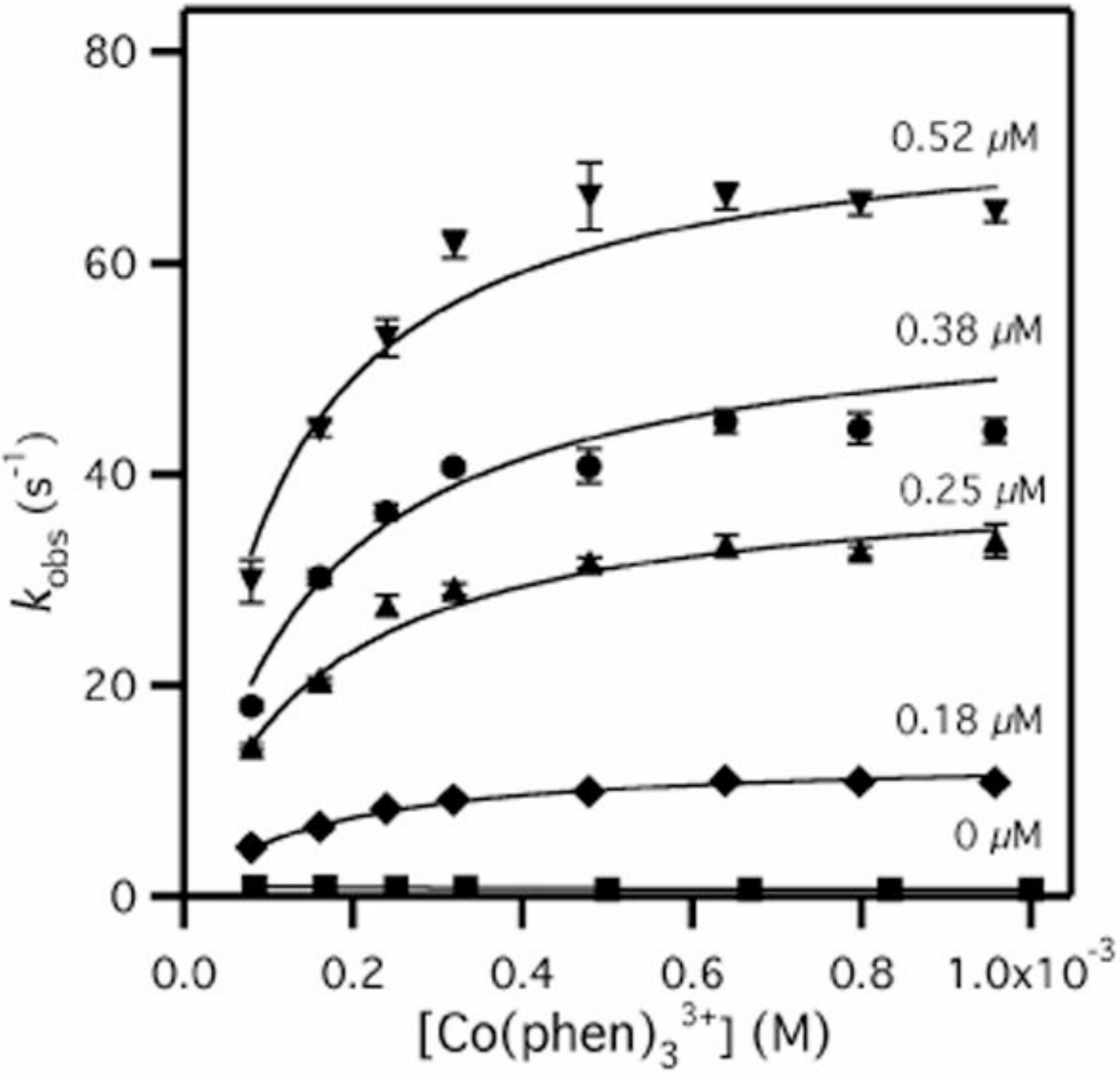

Figure 2.
Cyt *c* oxidation (5 μM) by $Co(phen)_3^{3+}$ in the presence of varied **Au-TAsp** (0 – 0.52 μM); buffer is 10 mM Tris, pH 7.40, 12 mM NaCl, *I* = 20 mM, 25.0°C.

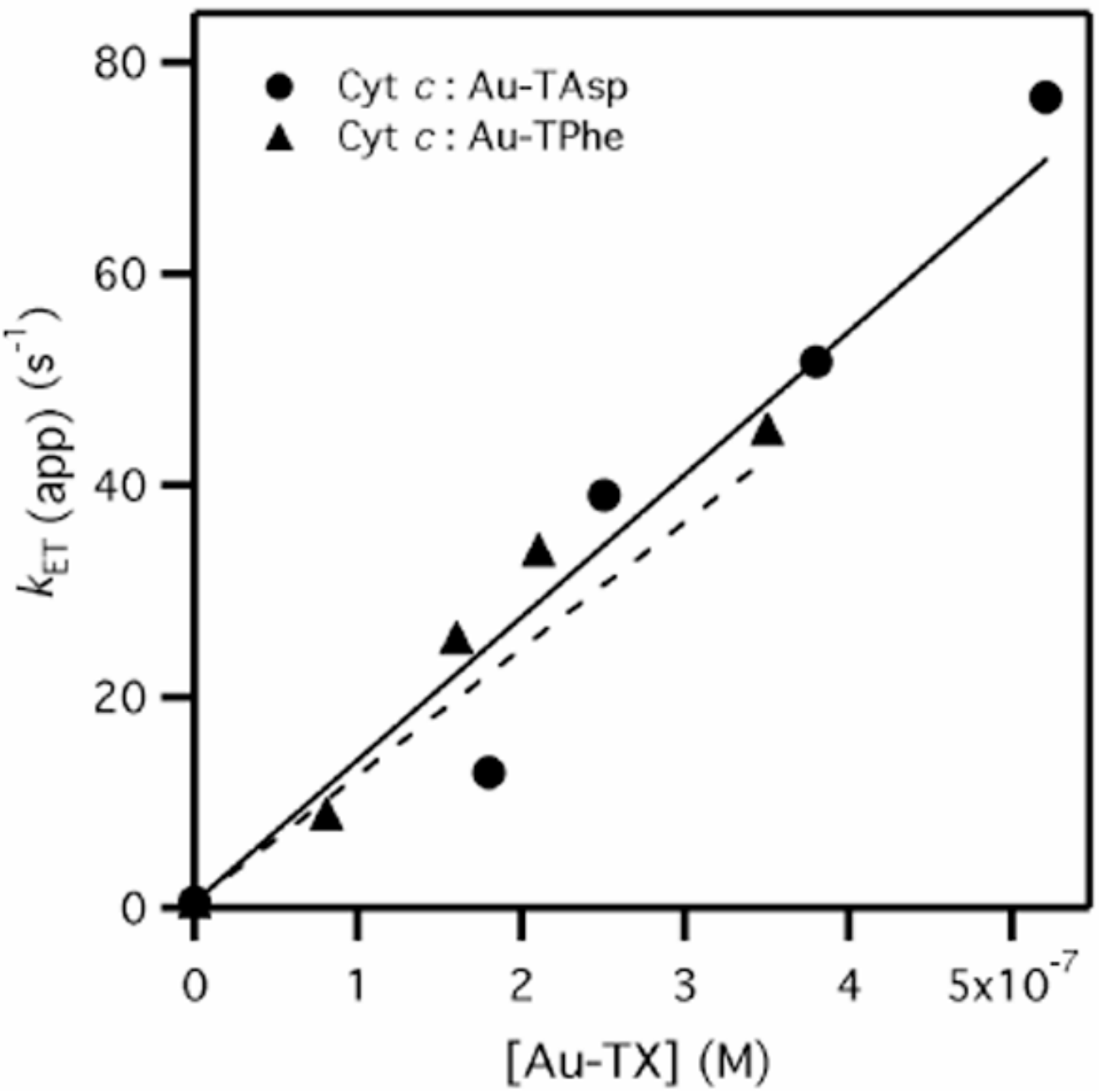

Figure 3.
Bimolecular rate plot for Cyt *c* oxidation (5 μM, 10mM Tris, pH 7.4, I = 20 mM) by Co(phen)$_3^{3+}$ in the presence of **Au-TX** (X = Asp, Phe). Linear fitting to (k_{ET}/K_S)[**Au-TX**] = $k_{ET(app)}$ yielded k_{ET}/K_S = 1.35 (±0.03) × 10^8 (X = Asp) and 1.20 (±0.03) × 10^8 M^{-1} s^{-1} (X = Phe). Error bars are approximately the size of each data point.